Supporting Information

Large π-conjugated tetrakis(4-carboxyphenyl) porphyrin enables high specific capacity and superior cycling stability in lithium-organic battery

Han Wu[a,b,=], Jianjun Zhang[b,=,*], Xiaofan Du[b], Min Zhang[b], Jinfeng Yang[b], Jinning Zhang[b], Ting Luo[a], Hao Liu[b], Hai Xu[a,*], Guanglei Cui[b,*]

[a] *College of Chemistry and Chemical Engineering， Central South University, Changsha 410083, P. R. China*

[b] *Qingdao Industrial Energy Storage Technology Institute, Qingdao Institute of Bioenergy and Bioprocess Technology, Chinese Academy of Sciences, Qingdao 266101, P. R. China.*

[=] *These authors contributed equally to this work.*

Corresponding author.

E-mail address: xhisaac@csu.edu.cn

zhang_jj@qibebt.ac.cn

cuigl@qibebt.ac.cn

Experimental Section

1.1 Materials:

Tetrakis (4-carboxyphenyl) porphyrin (TCPP) was synthesized according to previous reports with modifications. Pyrrole and methyl p-formylbenzoate was bought from Energy Chemical Company. Lithium difluoro(oxalate)borate (LiODFB) was supplied by Jiangsu Guotai Super Power New Materials Co., Ltd. Glass fibre was purchased from Whatman Co., Ltd. (UK). propylene carbonate (PC) was purchased from Macklin. Other reagents was commercially available.

For cell performance tests, the TCPP anode was prepared in a conventional casting method, by mixing 60 wt.% TCPP, 30 wt.% conductive carbon black (SuperP), and 10 wt.% PVDF. Finally, the specific density of active material on the electrodes was about 0.54 mg cm^{-2}. The galvanostatic charge/discharge tests of coin-type cells (CR2032) were conducted on LAND testing system (Wuhan LAND electronics Co., Ltd.) at room temperature.

1.2 Structural characterization:

^{1}H-NMR spectra of liquid samples were conducted on a nuclear magnetic resonance spectrometer (Bruker AVANCE-III 600), which was used to identify the structure of TCPP. Fourier transform infrared (FTIR) spectroscopy in the range of 4000 cm^{-1} - 400 cm^{-1}. X-ray diffractometer (SmartLab) was used to characterize sample structure. The TCPP anodes were characterized by scanning electron microscopy (SEM) (Hitachi S-4800, operating at 3 kV).

1.3 Electrochemical performance:

AC impedance spectroscopy were carried out on an electrochemical workstation (CHI660C, Shanghai Chenhua Co. China). AC impedance spectra was recorded in the frequency range from 1 mHz to 7×10^6 Hz at room temperature. Battery performance was performed on a LAND battery testing system (CT2001A, Wuhan LAND electronics Co., Ltd.). Coin cells (CR2032) were assembled in an argon-filled glove box(O_2 < 0.01 ppm, H_2O < 0.01 ppm).

1.4 Synthesis of 5,10,15,20–Tetrakis (4–methoxycarbonylphenyl) porphyrin (TPPCOOMe)

Pyrrole (6.0 mL, 0.086 mol) and methyl p-formylbenzoate (13.8 g, 0.084 mol) were added to refluxed propionic acid (250 mL) in a 500-mL three necked flask, and the solution was refluxed for 12 hrs. After the reaction mixture was cooled to room temperature, the solution was stored at -20 ^oC and left overnight to allow the precipitation of the porphyrins. The reaction solid was collected by filtration and washed by distilled water to remove the propionic acid. After re-crystal three times by chloroform ($CHCl_3$)/ethanol (volume ratio= 1:1) to yield purple crystals (TPPCOOMe). (4.3 g, 5.08 mmol, 24.3% yield). ^1H NMR (300 MHz, $CDCl_3$) δ 8.82 (s, 8H), 8.44 (d, 8H), 8.30 (d, 8H), 4.11 (s, 12H), -2.81 (s, 2H).

1.5 Synthesis of 5,10,15,20-Tetrakis (4-carboxyphenyl) porphyrin (TCPP)

The obtained TPPCOOMe (0.75 g) was stirred in tetrahydrofuran (THF) (25 mL) and methyl alcohol (MeOH) (25 mL) mixed solvent, to which a solution of potassium hydroxide (KOH) (2.63 g, 46.95 mmol) in distilled water (25 mL) was introduced. This mixture was refluxed for 12 hrs. After cooling down, THF and MeOH were evaporated. Additional water was added to the resulting water phase to fully dissolved the solid, then the mixture was neutralized with 1 M hydrochloric acid (HCl). The solid was collected by filtration, followed by washing three times with $CHCl_3$ and water separately, then dried in vacuum. ^{1}H NMR (300 MHz, $CDCl_3$) δ 13.28 (s, 4H), 8.86 (s, 8H), 8.39 (t, 16H), -2.91 (s, 2H).

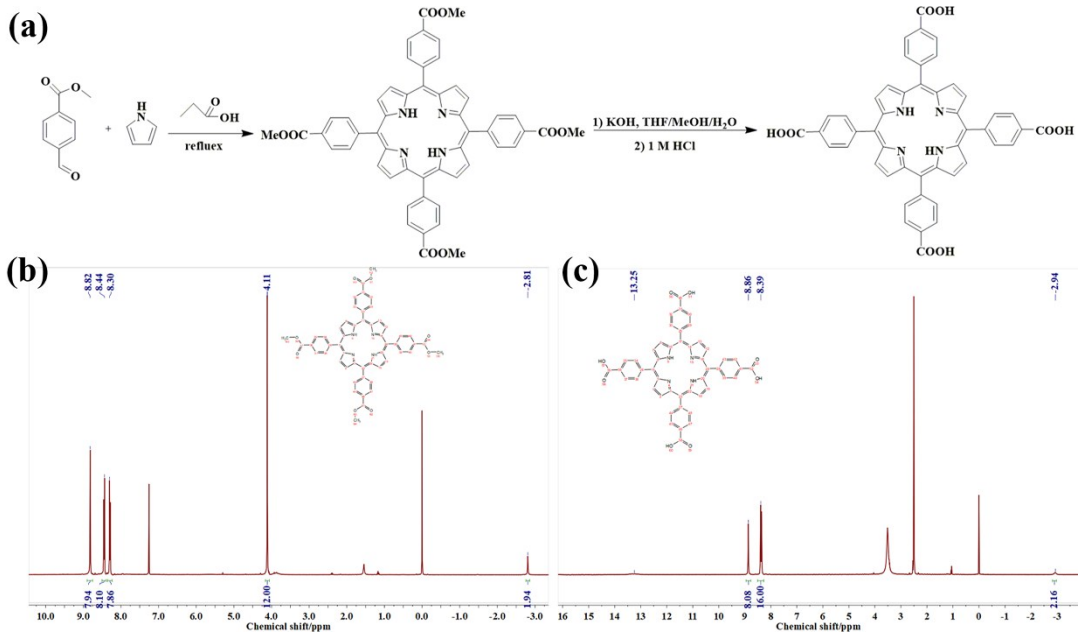

Fig. S1 Synthesis procedure and structural test of TCPP. (a) synthetic route of TCPP (b) 1H NMR spectra of TPPCOOMe. (c) 1H NMR spectra of TCPP.

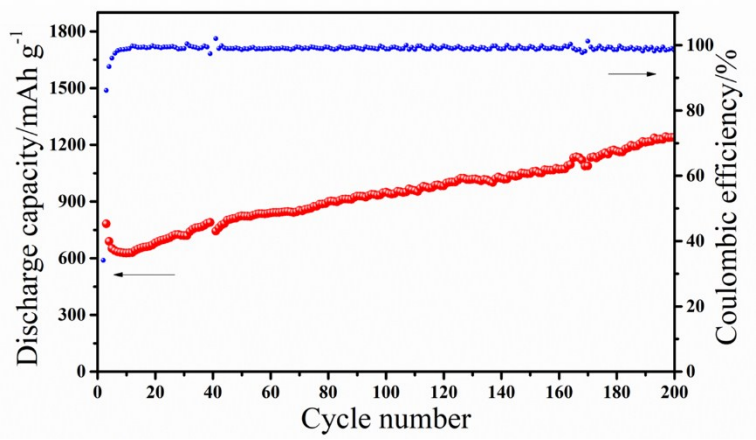

Fig. S2 Cycle performance of TCPP/Li at 358 mA g^{-1}

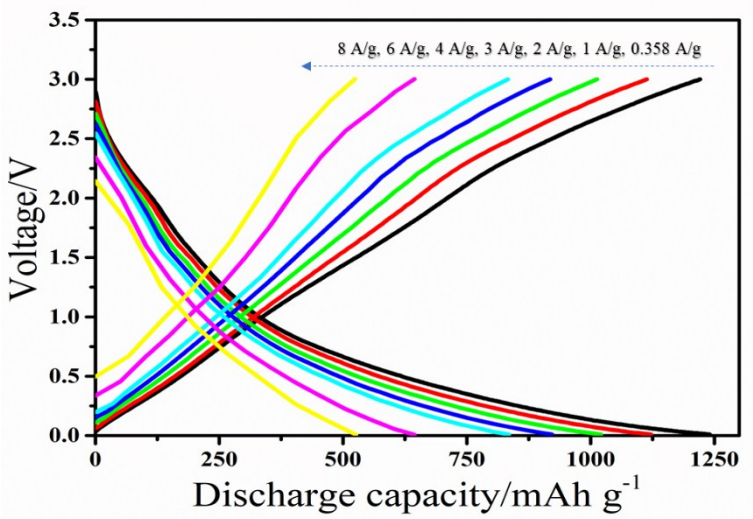

Fig. S3 Typical charge/discharge profiles of TCPP/Li battery at varied current density,

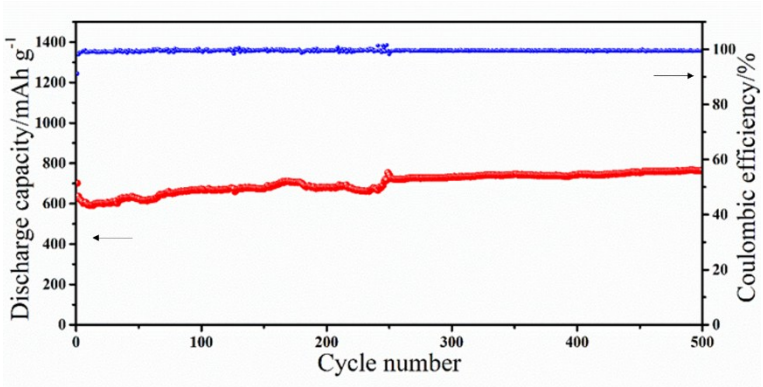

Fig. S4 Cycle performance of TCPP/Li battery at 2 A/g.

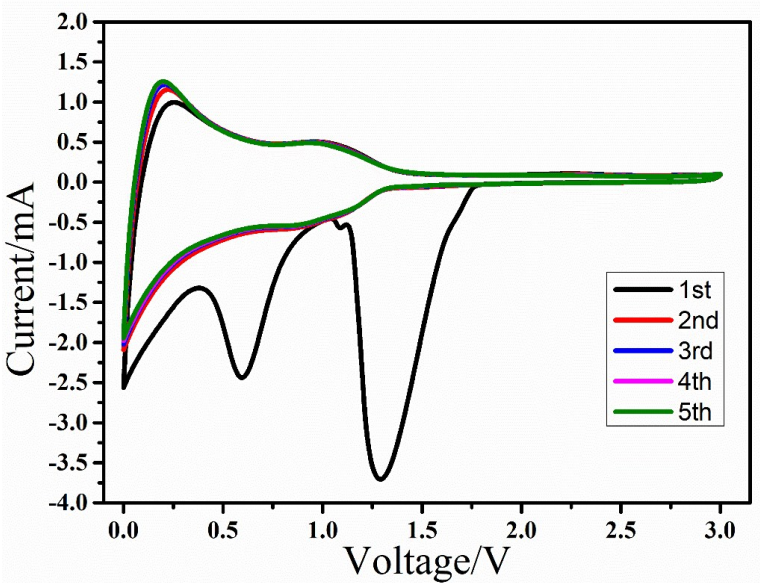

Fig. S5 Cyclic voltammograms of Super P/Li battery at voltage range of 0.01 V -3 V.

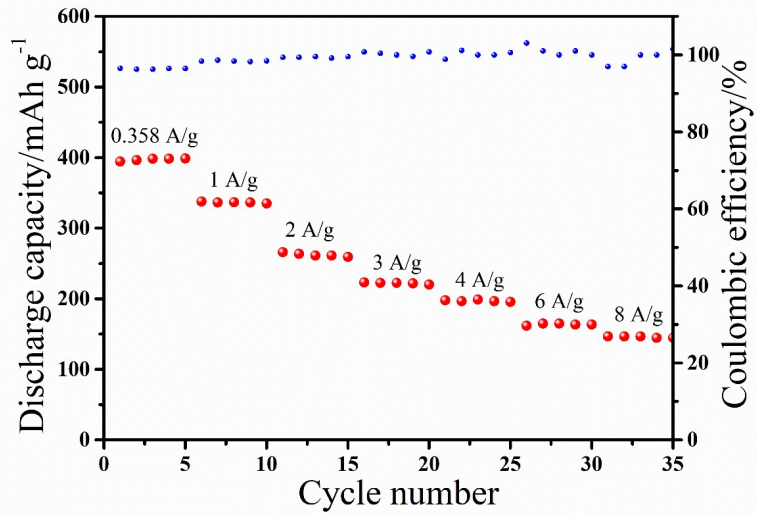

Fig. S6 Rate capability of Super P/Li battery at voltage range of 0.01 V -3 V.

.

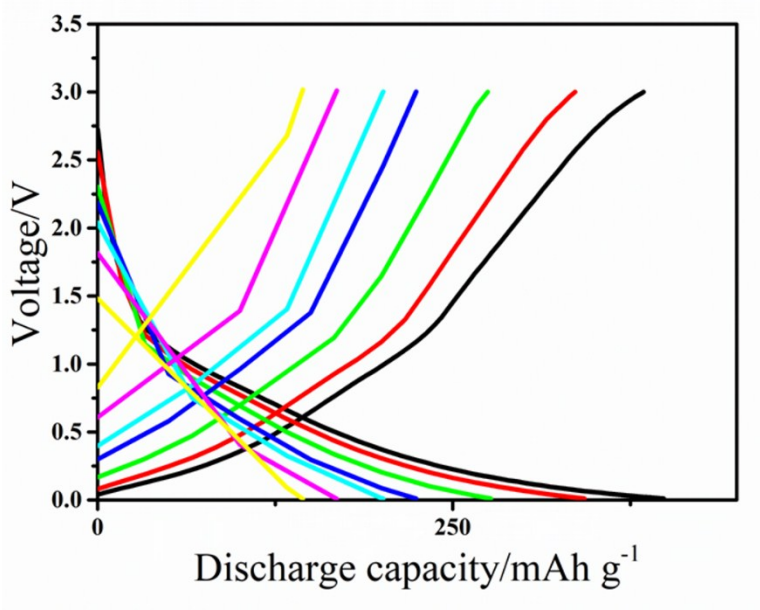

Fig. S7 Typical charge/discharge profiles of Super P/Li battery at varied current density,

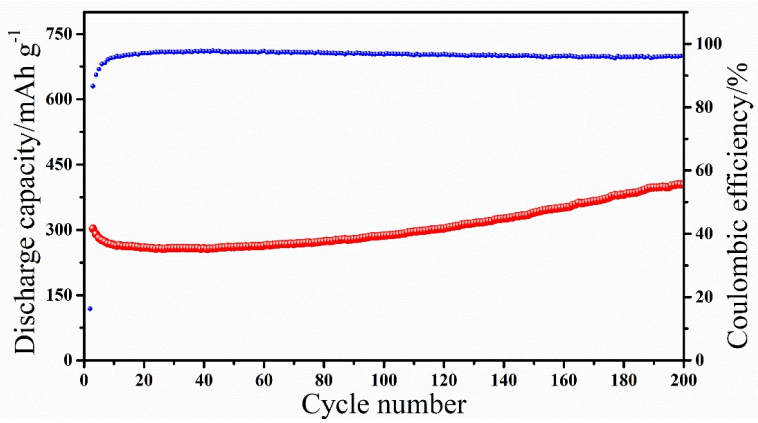

Fig. S8 Cycle performance of Super P/Li battery at 358 mA/g at voltage range of 0.01 V -3 V.

To eliminate the capacity provided by the Super P. The electrochemical performance of Super P was been texted at same condition. As it was shown in Figure S8, at current of 358 mA h g^{-1}, Super P deliver a capacity of ca. 400 mA h g^{-1} after 200 cycles. According to the literature, the capacity of 200 mA h g^{-1} (= 400 mA h g^{-1} × 30 wt.% of Super P / 60 wt.% of TCPP) was delivered from the conducting agent, Super P. The rate performance of Super P also been tested at same condition of TCPP anode. As it depicted in **Fig. S6** at 1, 2, 3, 4, 6, and 8 A g^{-1}, it provided 168.1, 130.6, 110.7, 87.8, 81.6 and 72.2 mA h g^{-1}, respectively.

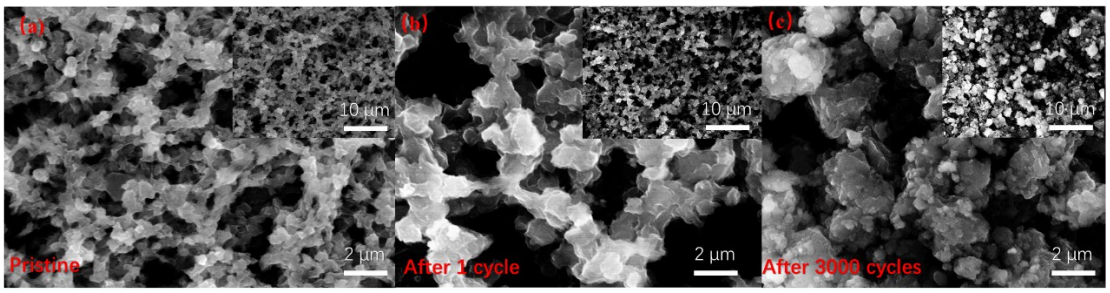

Fig. S9 Initial TCPP anode disassembled from TCPP/Li metal battery and after (e) 1 cycle (f) 3000 cycles.

The morphologies of TCPP electrode after different cycles were compared in **Fig. S9**. The shape of TCPP anode had no big change after 1 cycle, indicated TCPP was stable during the charge-discharge process. More importantly, even after 3000 cycles, the structure of TCPP was mostly preserved which also testify the superior cycling performance of TCPP electrode.

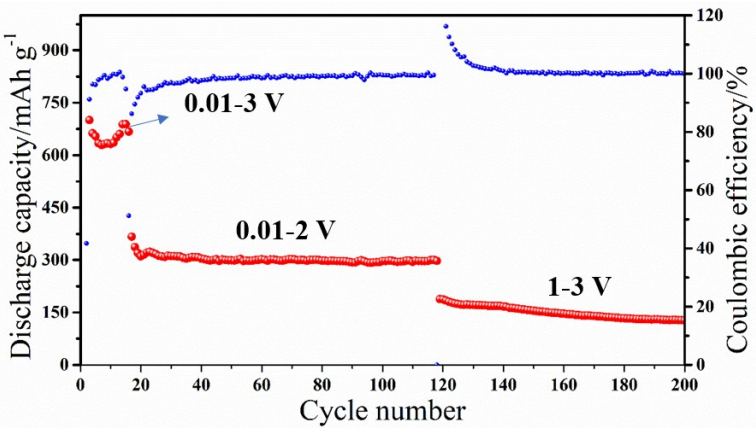

Fig. S10 Cycle performace of TCPP/Li battery at different voltage ranges.

To better evaluate the electrochemical performance of the TCPP anode, the influence of voltage range had been studied. **Fig. S10** depicted that after 15 cycles at voltage range from 0.01 to 3 V, when the voltage range narrowed to 0.01-2 V, the capacity dropped to ca. 300 mA h g^{-1}. This transformation should be ascribed to the release of some Li-ion which inserted into the π-conjugated system, and this process need a relatively high voltage and transformation from antiaromatic to aromatic states of the porphyrin occurred at voltage above 2 V. The capacity at higher range (1 - 3 V) were even worse than 0.01-2 V, about 160 mA h g^{-1}. This may be because that the insertion of Li-ion was mostly happened at voltage range below 1 V, as it was shown in the CV curves and discharge−charge profiles of TCPP anode.

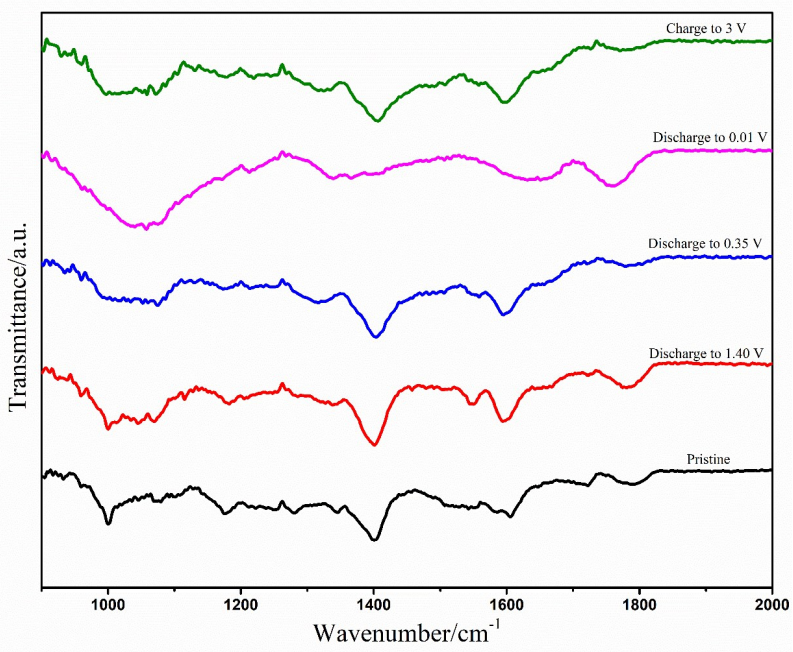

Fig. S11 Ex-situ FTIR spectra of TCPP anode in various charge/discharge states.

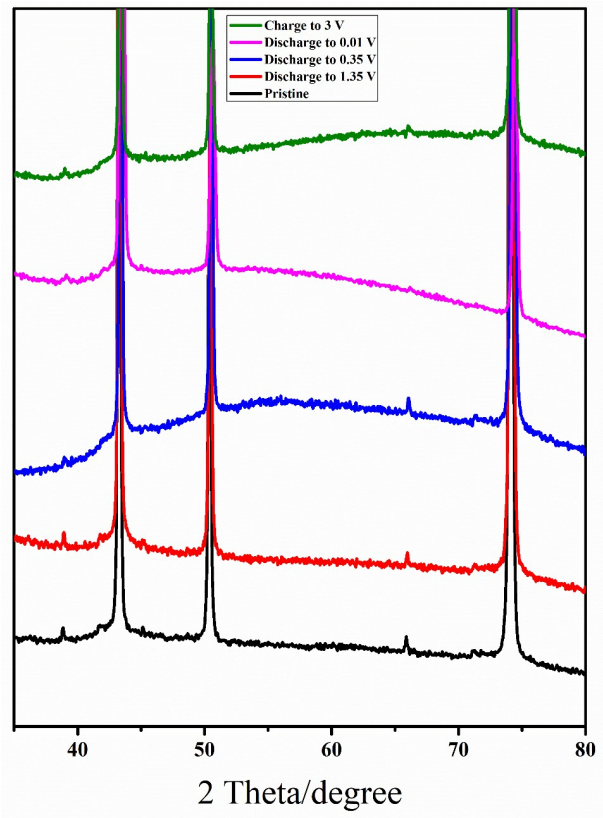

Figure S12 Ex-situ XRD patterns of TCPP anode in various charge/discharge states.

Table SI. Summary of main parameters and electrochemical performance of organic electrode materials.

Electrode material	High rate capacity [mAh g^{-1}] / discharge rate	Reversible capacity [mAh g^{-1}] / discharge rate	Capacity retention [%] /cycle number/ discharge rate	Voltage range	Note & reference
PIAQ	259 / 2 A g^{-1}	1231 / 200 mA g^{-1}	~79.3 / 1000 / 1 A g^{-1}	0-3.5 V	1
tetra-carboxyl- or octa-carboxyl-substituted phthalocyanines	-	586 / - 944 / -	~51.1 / 20 / - ~52.9 / 50 /-	0.3-3.2 V 0.3-3.2 V	2
DHCQ	207 / 5 A g^{-1}	921 / 50 mA g^{-1}	78 / 400 / 0.5 A g^{-1}	0.05-3 V	3
DASA	120 / 3 A g^{-1}	1100 / 50 mA g^{-1}	~95 / 1000 / 3 A g^{-1}	0.2-3 V	4
$C_8H_5Li_2NO_4$	-	237 / -	~84 / 50 / -	0.6-2 V	5
Co-LCP	168 / 1 A g^{-1}	545 / 50 mA g^{-1}	~03 / 50 / 0.05 A g^{-1}	0.1-3 V	6
PDA derivative	~1100 / 3.2 A g^{-1}	1818 / 50 mA g^{-1}	93 / 580 / 0.5 A g^{-1}	0.1-3 V	7
TThPP	~195 / 4 A g^{-1}	666 / 50 mA g^{-1}	61.1 / 200 / 1 A g^{-1}	0.05-3 V	8
PSB	40.3 / 0.08 A g^{-1}	175 / 10 mA g^{-1}	90 / 100 / 0.01 A g^{-1}	0.01-3.5 V	9
F-HBC	100 / 7 A g^{-1}	200 / 1000 mA g^{-1}	More than 100% / 400 / 1 A g^{-1}	0.01-3 V	10
Maleic acid	570.8 / 46.2 A g^{-1}	1500 / 46.2 mA g^{-1}	98.1 / 500 / 2.31 A g^{-1}	0.01-3 V	11
TCPP*	548.4 / 8 A g^{-1}	1200 / 358 m A g^{-1}	More than 100% / 200 / 0.358 A g^{-1} More than 100% / 500 / 2 A g^{-1} 80.5 / 3000 / 6 A g^{-1}	0.01-3 V	

Reference

1 Z. Man, P. Li, D. Zhou, R. Zang, S. Wang, P. Li, S. Liu, X. Li, Y. Wu, X. Liang, *J. Mater. Chem. A,* 2019, **7**: 2368.

2 J. Chen, Q. Zhang, M. Zeng, N. Ding, Z. Li, S. Zhong, T. Zhang, S. Wang, G. Yang, *J. Solid State Electrochem*., 2016, **20**: 1285.

3 L. Chen, S. Liu, L. Zhao, Y. Zhao, Electrochimica Acta, 2017, **258**: 677.

4 D. Mukherjee, G. Gowda Y. K, H. Makri Nimbegondi Kotresh, S. Sampath, *ACS Appl. Mater. Inter*., 2016, **9**: 19446.

5 S. Renault, V. A. Oltean, M. Ebadi, K. Edström, D. Brandell, *Solid State Ionics*, 2017, **307**: 1.

6 C. Shi, Q. Xia, X. Xue, Q. Liu, H.-J. Liu, *RSC Adv.*, 2016, **6**: 4442.

7 T. Sun, Z. j. Li, H. g. Wang, D. Bao, F. l. Meng, X. b. Zhang, *Angew. Chem. Int. Edit*, 2016, **55**: 10662.

8 H. Yang, S. Zhang, L. Han, Z. Zhang, Z. Xue, J. Gao, Y. Li, C. Huang, Y. Yi, H. Liu, *ACS Appl. Mater. Inter.*, 2016, **8**: 5366.

9 H. Ye, F. Jiang, H. Li, Z. Xu, J. Yin, H. Zhu, *Electrochimica Acta*, 2017, **253**: 319.

10 J. Park, C. W. Lee, J. H. Park, S. H. Joo, S. K. Kwak, S. Ahn, S. J. Kang, *Adv. Sci*., 2018, **5**: 1801365.

11 Y. Wang, Y. Deng, Q. Qu, X. Zheng, J. Zhang, G. Liu, V. S. Battaglia, H. Zheng, *ACS Energy Letters*, 2017, **2**: 2140.